CALORIMETRY WITH FLASH CHAMBERS

D. Bogert, R. Burnstein*, R. Fisk, S. Fuess, J. Morfin,
T. Ohska, M. Peters†, L. Stutte, J.K. Walker, H. Weerts
Fermi National Accelerator Laboratory
Batavia, Illinois

J. Bofill, W. Busza, T. Eldridge, J.I. Friedman,
M.C. Goodman, H.W. Kendall, T. Lyons, R. Magahiz,
T. Mattison, A. Mukherjee, L. Osborne, R. Pitt,
L. Rosenson, A. Sandacz, M. Tartaglia, R. Verdier,
S. Whitaker, G.P. Yeh
Massachusetts Institute of Technology
Cambridge, Massachusetts

M. Abolins, R.Brock, A. Cohen, J. Ernwein#,D. Owen,
J. Slate
Michigan State University
E. Lansing, Michigan

F.E. Taylor
Northern Illinois University
DeKalb, Illinois

October 1982

Presented by S. Fuess; Gas Sampling Calorimetry Workshop

* permanent address: Illinois Institute of Technology
Chicago, Illinois
† permanent address: University of Hawaii, Honolulu, Hawaii
# permanent address: CEN, Saclay, France

Abstract:

The flash chambers used in the Fermilab E594 neutrino experiment are described, and their use in a calorimeter discussed. Resolutions obtained with a calibration beam are presented, and comments made about the pattern recognition capabilities of the calorimeter.

Introduction:

A large neutrino detector requires an economical method of achieving uniform fine grain sampling of the final state shower to achieve good energy and spatial resolution. Experiment E594 at Fermilab has successfully used flash chambers as the basis of a neutrino calorimeter.

Flash chambers are digital devices: a cell in a chamber can record only the presence of an ionizing particle. Calorimetry is done by using many cells in many chambers, sampling an electromagnetic or hadronic shower many times laterally and longitudinally. The energy of the shower is obtained from the total number of hit cells; the angle of the shower is obtained from the alignment of the hit cells. Additional details of the shower structure are available.

Flash Chamber Construction:

The E594 flash chambers are constructed from extruded polyproplyene sheets, with 5 mm by 5.9 mm rectangular cells. The chambers are built in 3 views, with the cells at 0°, 80°, and 100° from the horizontal. Each chamber is constructed from three 4' wide panels of black polypropylene sheets to form a total sensitive area of 12' by 12' with roughly 650 cells. Figure 1 shows the construction of a chamber with horizontal cells. The polypropylene sheet is fitted with gas manifolds at each end, and a mixture of 90% neon and 10% helium flows through the cells at a rate of approximately one volume change per hour. High voltage electrodes of 5 mil aluminum foil are glued to both sides of the polyproplyene sheet. When a charged particle of interest traverses the chamber a high voltage pulse is applied to the electrodes, creating a high electric field within the polyproplyene sheet. The avalanche in the traversed cell initiated by the high electric field creates a plasma discharge which propagates down the cell. To eliminate cell-to-cell cross talk, the electrodes extend only to within one foot of the cell ends. The plasma discharge is thus quenched before it reaches the gas manifold.

The high voltage pulse is produced on each chamber by a pulse forming network (PFN) with a characteristic impedance of 5 ohms. Figure 2 shows the PFN circuit. The capacitance of the PFN is distributed in three stages, with larger

capacitance in the first stage to insure a good rise time. The PFN is triggered by a spark plug which acts as a switching element. A typical high voltage pulse has a rise time of approximately 60 nsec, an amplitude of 5 kV, and a duration of 500 nsec. The plasma propagation speed with these conditions is found to be roughly 0.1 foot/nsec.

The flash chambers are read out by using magnetostrictive wire techniques to detect the current pulse induced by the plasma in a struck cell. Figure 3 shows the readout region in detail. Copper strips 3 mm wide and 508 mm long are glued to the polyproplyene surface near the end of the cells. The strips are constructed by photoetching copper clad mylar sheets. The strips are connected to the chamber ground electrode via "sense" wires and form a set of capacitors with the high voltage electrode. The plasma discharge in a struck cell causes the capacitance between the readout strip and the high voltage electrode to change, inducing a current pulse to flow through the copper strips to the ground electrode.

The chamber ground electrode lies over the photoetched strips, insulated by an additional layer of 5 mm thick polyproplyene. The layer of polyproplyene reduces the shunt capacitance between the copper strips and the ground plane. Unwanted capacitive pickup in strips above unstruck cells is reduced by means of a type of A C bridge. A 2" wide "bucking strip" is placed perpendicularly across all of the copper

strips. The bucking strip is connected on one end to the high voltage electrode of the chamber through a 1:1 inverting cable transformer and a resistance R_1; it is connected on the other end to the chamber ground plane through a resistance R_2. The proper choice of the resistors, determined from the chamber geometry, reduces the unwanted pickup by a factor of 3 to 4.

A 5 by 12 mil Remendur 27 magnetostrictive (m.s.) wire is placed over the sense wire region. The current pulse induced in the sense wire of a struck cell induces an acoustic pulse on the m.s. wire. The acoustic pulse propagates along the m.s. wire at roughly 5000 m/sec, providing a 1 μsec separation of adjacent hit cells. The m.s. wire is held in a 10 mil deep groove in a long aluminum bar (wand). A solenoidal coil is wound along the entire length of the wand to periodically magnetize the m.s. wire. It has been found that there is an optimum magnetization of the m.s. wire minimizing dispersion and limiting attenuation of the acoustic pulse to roughly 20% per 6 feet.

Amplifiers with gains of roughly 10^3 at each end of the wand provide analogue signals for the readout system. Three fiducial marks, in the center and at the ends of the wand, are created by placing wires connecting the high voltage and ground electrodes across the m.s. wire. Typical pulse amplitudes from hit cells are 100 to 200 mV. A signal to noise ratio of 10:1 to 20:1 is achieved. Figure 4 shows a

detailed section of the signal observed after amplification for a number of different pulses. The spike on the right edge of each trace is a fiducial. Single and multiple hits are clearly distinguishable.

Each amplifier signal feeds a discriminator circuit, which in turn clocks signals into a 1024 by 1 memory. The discriminator is programmed with an exponentially decreasing threshold to compensate for the attenuation of the signal along the m.s. wire. The memory boards are read out asynchronously by CAMAC into a PDP-11 computer.

Flash Chamber Calorimetry: [2]

The E594 neutrino detector, illustrated in Figure 5, consists of a target - calorimeter and a muon spectrometer. The muon spectrometer consists of three 24' diameter and four 12' diameter iron toroids, instrumented with proportional planes. The calorimeter is constructed of 38 modules, also illustrated in Figure 5. Each module contains 16 flash chambers in alternating orientations, 5/8" thick acrylic plastic extrusions filled alternatively with sand and steel shot, and a single proportional tube plane. The sand and steel shot provide the target mass, totalling 340 tons for the entire calorimeter. The proportional tube planes, aligned alternatively between horizontal and vertical, provide a trigger as well as an independent

measure of the shower energy. Liquid scintillation counters are placed every 5 modules to provide a high efficiency fast timing signal.

The average density of the calorimeter is 1.4 g/cm^3; the average Z is 21. Flash chambers sample every 22% of a radiation length and every 3% of an interaction length. Proportional tubes sample every 3.5 radiation lengths and every 50% of an interaction length. The low density and the low Z of the calorimeter are important for good energy flow measurements of hadron showers.

Figure 6 illustrates a neutrino induced event in the calorimeter. The event is observed in the three orientations of the flash chambers, with each hit cell being represented by a dot. The bar graphs at the top and the bottom of the figure display the pulse heights in the proportional tube planes which provided the trigger for this event. There are approximately 1800 struck cells in the hadronic shower, corresponding to an energy of roughly 50 GeV. The toroids are shown at the right of Figure 6; the "+" signs indicate hits in the proportional tube planes between toroids.

Resolutions:

From an exposure to a calibration beam we have determined the detector response to particles of known energy and direction. The calibration beam contained hadrons, muons, or electrons identified with a Cerenkov counter. The energy range was from 5 to 125 GeV.

Figure 7 shows the observed number of hit cells as a function of incident particle energy. At high energies the response becomes nonlinear. This is a result of the saturation of the flash chambers, in which more than one particle traverses a single cell. By determining the local density of hit cells, this saturation may be statistically corrected. The corrected number of hit cells, also shown in Figure 7, now responds linearly over the energy range of interest.

Figure 8 presents the energy and angle resolutions obtained with the calibration beam. Electron shower angles were computed by a weighted least squares method using the flash chamber hit cell information. The weights used in the fit were determined from average shower characteristics and the statistics associated with hit cells. Hadron angles were similarly computed, but with a different weighting scheme determined by much larger fluctuations in shower structure. Muon angles were computed with a least squares procedure with a weighting along the track determined by multiple scattering.

Electron and hadron energies are computed by counting the number of hit cells associated with the shower. The saturation of the flash chambers has been accounted for by estimating the actual number of particles from the observed density of hit cells. At very high shower energies, the energy resolution of the proportional tubes becomes better than that of the flash chambers alone. The dashed line in Figure 8 shows the estimated energy resolution for high energy electrons as determined by the proportional tubes.

Pattern Recognition:

The fine grain sampling of the final state shower by the flash chambers allows for excellent pattern recognition capabilities. Charged and neutral current separation is aided by the identification of a long straight track as a muon. Details of the shower structure also aid in event identification. Figure 9a displays a magnified (8 modules are shown) calibration beam electron, as identified by a Cerenkov counter. The electron has a characteristically high density of hit cells and a lack of identifiable individual tracks. Figure 9b displays a calibration beam hadron (12 modules are shown). The hadron shower has clearly distinguishable individual tracks, and is in general less dense than the electron shower. The separation of electromagnetic and hadronic showers can be made by

exploiting the ability of the detector to recognize shower features to a fine level.

Summary:

A fine-grained neutrino detector with flash chambers has been operated at Fermilab. The detector has excellent energy and angle resolution, and unique pattern recognition capabilities. Data has been taken during a wide band neutrino beam engineering run and during a narrow band neutrino beam exposure. We look forward to using the detector to explore neutrino physics at TeV energies.

References:

1) F.E. Taylor et al.; IEEE NS-25, 312 (1978).

F.E. Taylor et al.; IEEE NS-27, 30 (1980).

2) L. Stutte, et al.; "Early Results from E-594, A Fine Grained Neutrino Detector", Proceedings of the 1981 International Conference on Neutrino Physics and Astrophysics, Maui, Hawaii, July 1-8, 1981.

D. Bogert, et al.; "The Operation of a Large Flash Chamber Neutrino Detector at Fermilab", IEEE NS-29, 363 (1982).

Figure Captions

Figure 1 : Details of the construction of a flash chamber.

Figure 2 : The Pulse Forming Network and a typical HV pulse.

Figure 3 : Construction of the readout section.

Figure 4 : Typical pulses from the wand amplifier without and with the bucking circuit.

Figure 5 : Layout of the detector and details of an individual module.

Figure 6 : A neutrino induced event in the detector.

Figure 7 : Number of hit cells as a function of incident particle energy.

Figure 8 : Angle and energy resolutions.

Figure 9a: An electron shower.
9b: A hadron shower.

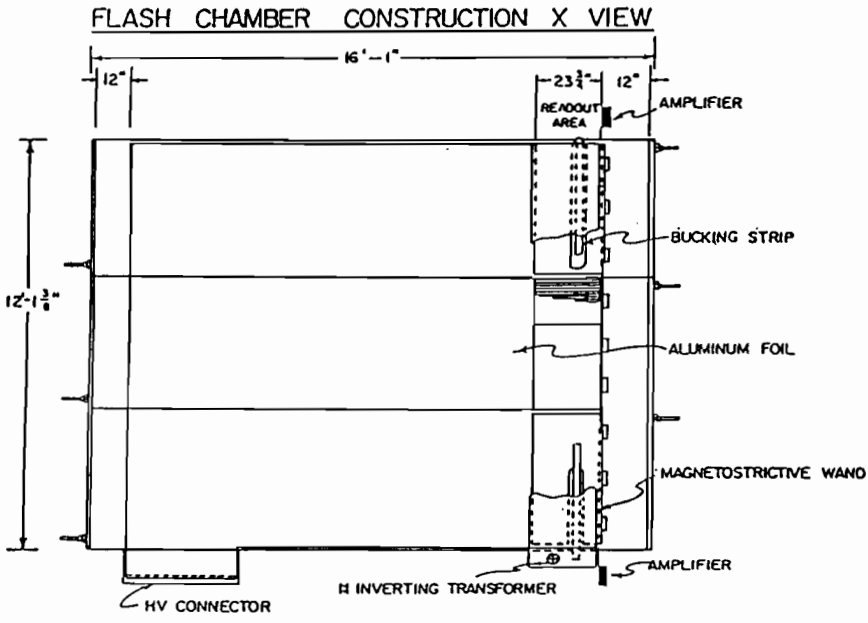
FLASH CHAMBER CONSTRUCTION X VIEW
16'-1"
12"
23 3/4"
12"
READOUT AREA
AMPLIFIER
BUCKING STRIP
12'-1 3/8"
ALUMINUM FOIL
MAGNETOSTRICTIVE WAND
AMPLIFIER
INVERTING TRANSFORMER
HV CONNECTOR

Figure 1

THE HIGH VOLTAGE PULSE FORMING NETWORK

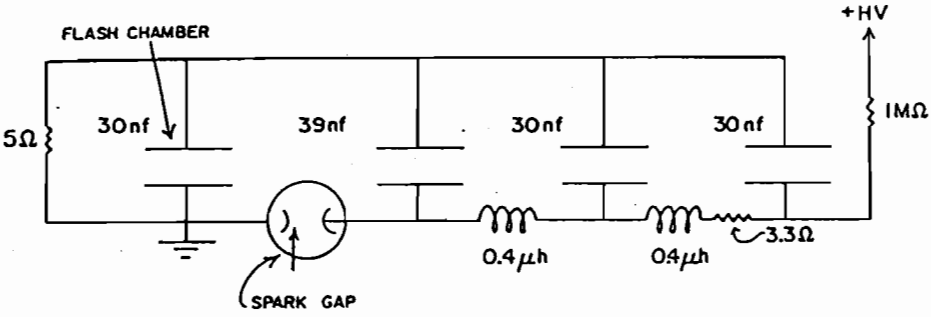

HIGH VOLTAGE PULSE

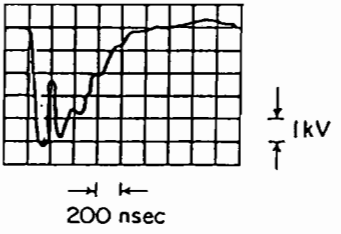

Figure 2

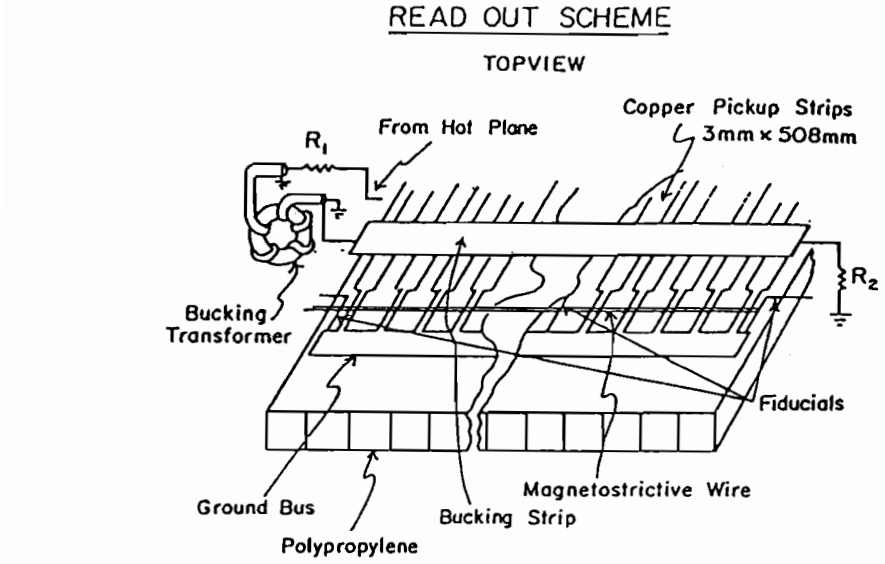
READ OUT SCHEME
TOPVIEW
Copper Pickup Strips
3mm x 508mm
From Hot Plane
R_1
R_2
Bucking
Transformer
Fiducials
Ground Bus
Polypropylene
Bucking Strip
Magnetostrictive Wire

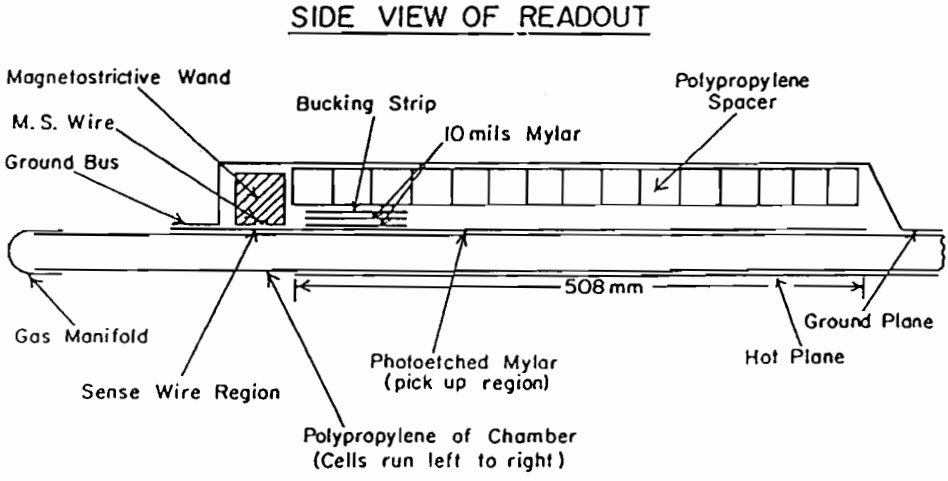
SIDE VIEW OF READOUT
Magnetostrictive Wand
M. S. Wire
Ground Bus
Bucking Strip
10 mils Mylar
Polypropylene
Spacer
508 mm
Gas Manifold
Sense Wire Region
Photoetched Mylar
(pick up region)
Polypropylene of Chamber
(Cells run left to right)
Ground Plane
Hot Plane

Figure 3

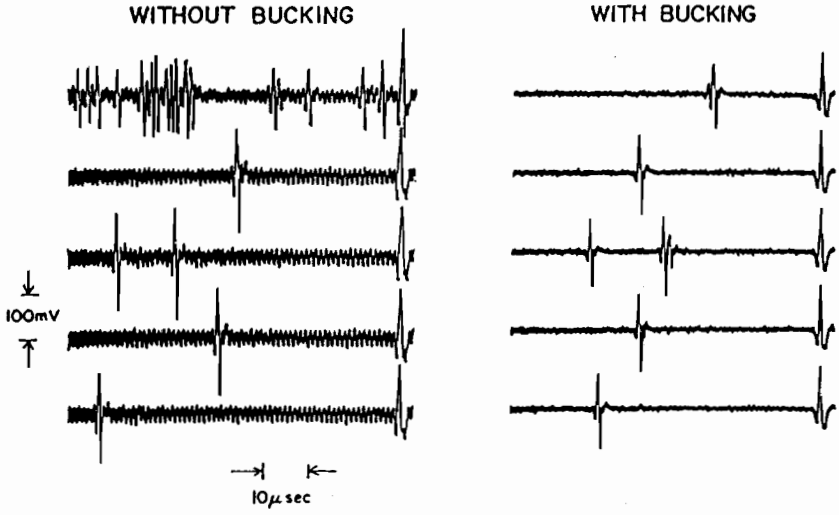

Figure 4

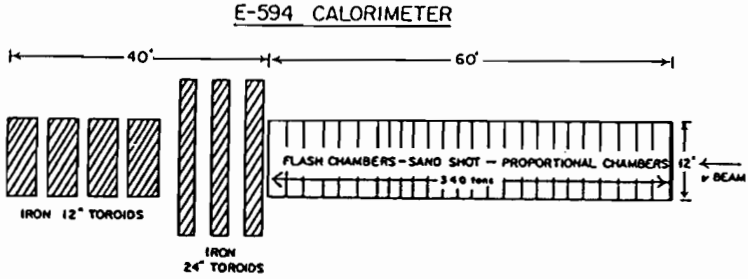
E-594 CALORIMETER
40'
60'
FLASH CHAMBERS - SAND SHOT - PROPORTIONAL CHAMBERS
340 tons
12'
BEAM
IRON 12" TOROIDS
IRON
24" TOROIDS

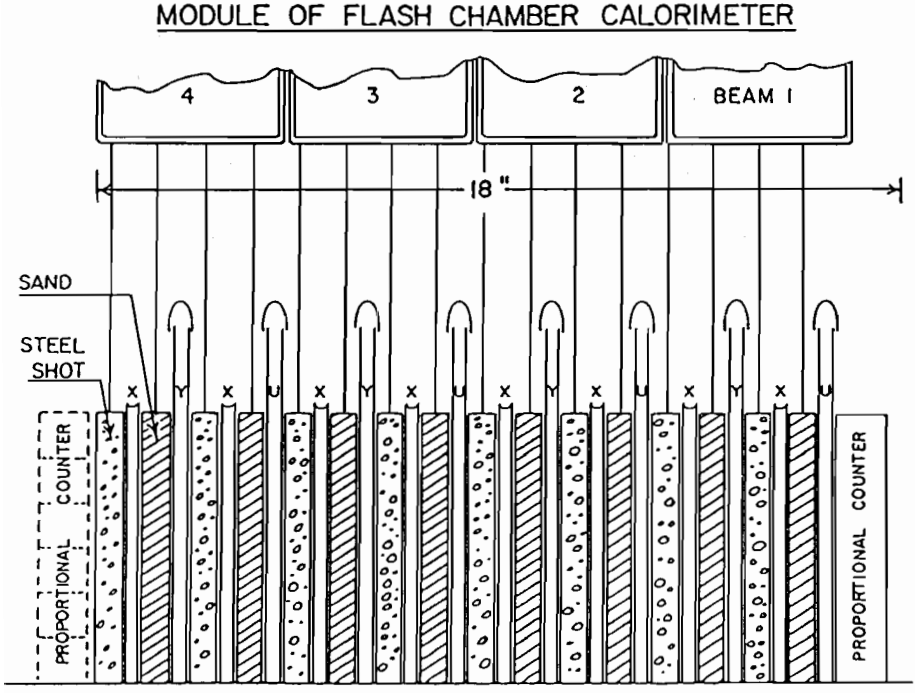
MODULE OF FLASH CHAMBER CALORIMETER
4
3
2
BEAM 1
18"
SAND
STEEL
SHOT
PROPORTIONAL COUNTER
PROPORTIONAL COUNTER

Figure 5

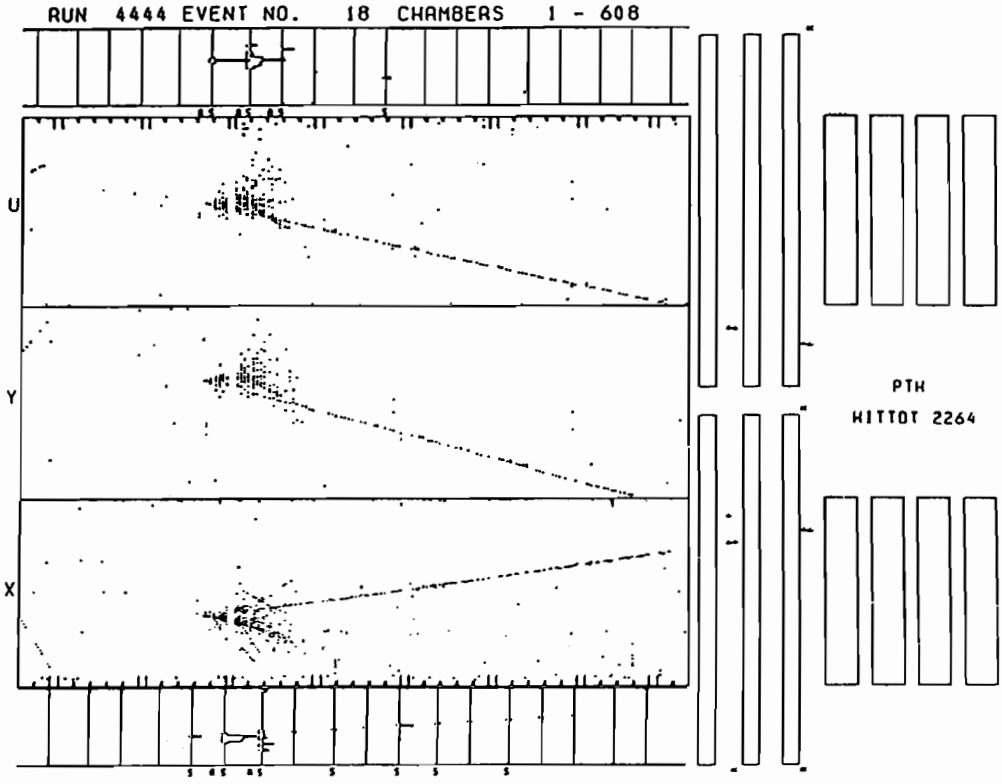

Figure 6

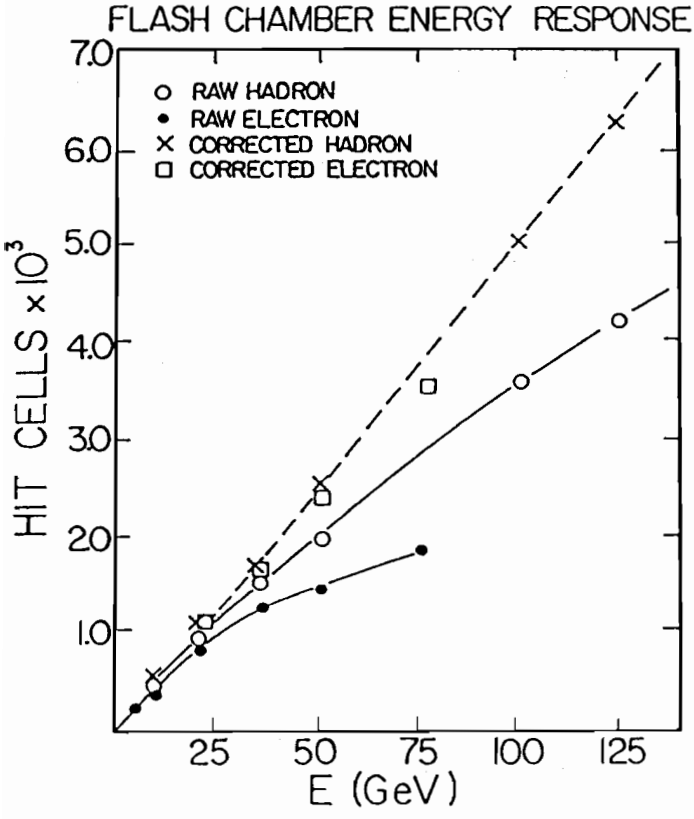
FLASH CHAMBER ENERGY RESPONSE
RAW HADRON
RAW ELECTRON
CORRECTED HADRON
CORRECTED ELECTRON
HIT CELLS x 10³
7.0
6.0
5.0
4.0
3.0
2.0
1.0
25
50
75
100
125
E (GeV)

Figure 7

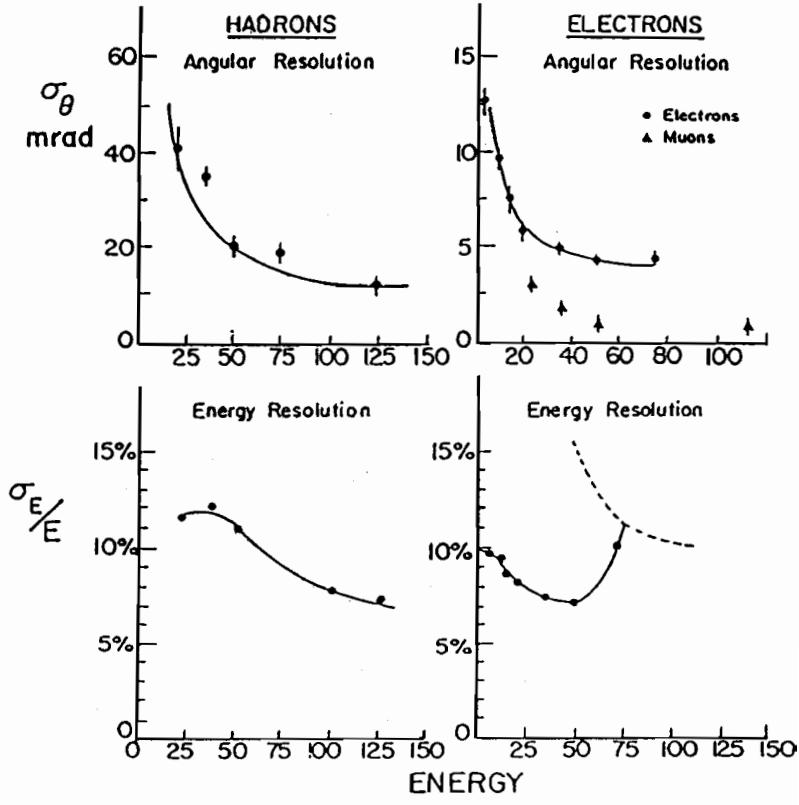
HADRONS
Angular Resolution
σ_θ
mrad
60
40
20
0
25 50 75 100 125 150
ELECTRONS
Angular Resolution
Electrons
Muons
15
10
5
0
20 40 60 80 100
Energy Resolution
$\sigma_{E/E}$
15%
10%
5%
0
0 25 50 75 100 125 150
Energy Resolution
15%
10%
5%
0
25 50 75 100 125 150
ENERGY

Figure 8

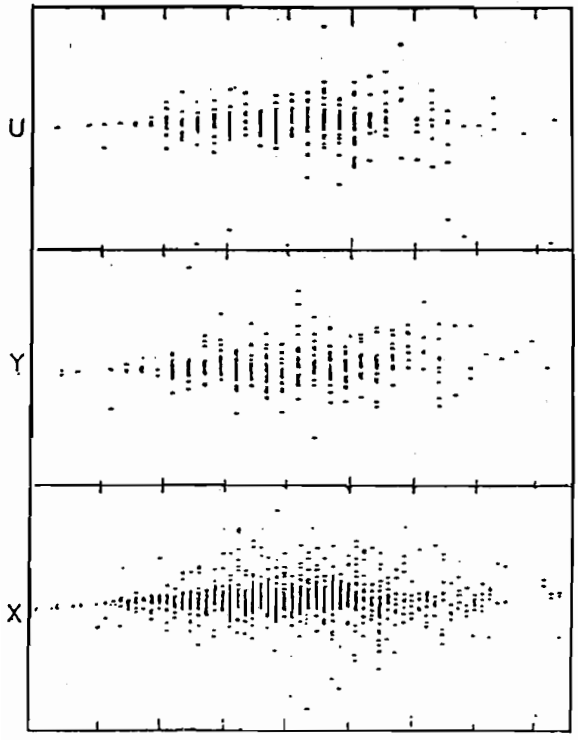

Figure 9a

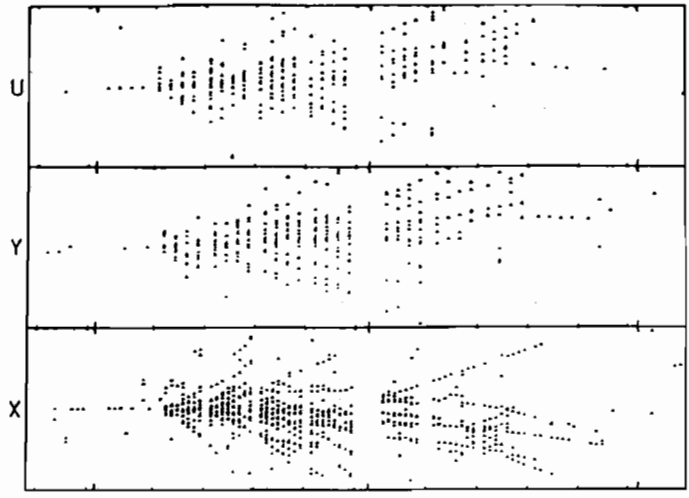

Figure 9b